Integral Analysis of Transonic Shock Wave/Boundary-Layer Interaction in Internal Flow

Deepak Om* and Morris E. Childs†
University of Washington, Seattle, Washington

An approximate integral viscous-inviscid interaction method is presented for calculating the development of a turbulent boundary layer subjected to a normal shock wave in an internal flow. The inflow conditions and the downstream pressure are provided for the computation. In the supersonic region of shock pressure rise, the Prandtl-Meyer function is used to couple the viscous and inviscid flows. An analytical model for the coupling process is postulated and appropriate equations are defined. Downstream of the sonic point, one-dimensional inviscid flow is assumed for coupling with the viscous flow. The viscous flow is calculated using Green's integral lag-entrainment boundary-layer method. Comparisons of the solutions with the experimental data are made for interactions which are unseparated, near separation, and separated. For comparison purposes, solutions to the time-dependent, mass-averaged Navier-Stokes equations incorporating a two-equation, Wilcox-Rubesin turbulence model are also presented. The computed results from the integral method show good agreement with experimental data for unseparated interactions and reasonable agreement with the trend of the viscous effects when the interaction becomes increasingly separated.

Nomenclature

C_E = entrainment coefficient
C_f = skin-friction coefficient, $2\tau_w/\rho_e u_e^2$
C_τ = shear-stress coefficient
F = function of C_E and C_f
$H, H_1, \bar{H}$ = velocity profile shape parameters
H_k = kinematic value of H
M = Mach number
n = exponent in ν_{ref} model
P = pressure
R = radius of the duct
Re = Reynolds number
T = temperature
u = streamwise velocity
x = axial distance
$\bar{X}$ = $(x-x_u)/\delta_u$
Δ = mass-flow thickness
δ = boundary-layer thickness
δ^* = boundary-layer displacement thickness
γ = specific heat ratio (= 1.4)
θ = boundary-layer momentum thickness
λ = scaling parameter for secondary influences on turbulence structure
ν = Prandtl-Meyer function
ρ = density
τ = shear stress
ϕ = flow angle at the boundary-layer edge

Subscripts

0 = stagnation condition
EQ = equilibrium conditions
EQ_0 = equilibrium conditions in absence of secondary influence on turbulence structure
e = boundary-layer edge
F = $\nu_{\text{ref}} = 0$
r = recovery condition
ref = reference condition
u = start of interaction
∞ = freestream condition at the start of interaction

Presented as Paper 83-1402 at the AIAA/SAE/ASME 19th Joint Propulsion Conference, Seattle, WA, June 27-29, 1983; received Nov. 26, 1984; revision received April 15, 1985.

*Research Assistant Professor, Dept. of Mechanical Engineering; currently with Boeing Commercial Airplane Company, Seattle, WA. Member AIAA.

†Professor, Department of Mechanical Engineering. Member AIAA.

I. Introduction

TRANSONIC normal shock wave/turbulent boundary-layer interactions represent an important problem in fluid mechanics because of the frequent occurrence of such interactions in both external flows (e.g., on wings in transonic flight) and internal flows (e.g., in the inlet of air-breathing engines). In internal interactions, the flow blockage due to the wall boundary layers produces a flowfield that is different from that occurring in external flows.[1-3] The effect of blockage is to produce a lower pressure recovery, a less retarded boundary-layer flow, and a larger embedded supersonic region.[3] (The embedded supersonic region was termed "supersonic tongue" by Seddon.[1])

In the last few years, there have been significant advances in the development of viscous-inviscid interaction techniques as demonstrated at the AGARD Conference.[4] Most of the techniques developed for application to transonic shock wave/turbulent boundary-layer interactions employ integral methods for the boundary-layer and finite-difference schemes for the inviscid flow. One approach to the solution of such interactions is to solve the inviscid flow and the viscous flow and couple the two. A large portion of the computing time usually is spent in calculating the shock-embedded transonic inviscid flows. A simple analysis of such interactions is important for design purposes. One of the main objectives of any design analysis is to minimize the computing time so that a code can be used to compute perhaps hundreds of such interactions to achieve a given design.

In this paper, an analytical model is postulated for coupling the viscous and inviscid flows that eliminates the computation of the shock-embedded inviscid internal transonic flow, thus reducing the computing time. The objective of the

present analysis is to calculate the development of the turbulent boundary layer subjected to a normal shock wave in an internal flow. The present analysis is applicable to both planar and axisymmetric internal flows. The results presented here are only for axisymmetric flows, since data obtained for axisymmetric interactions are known to be free from undesirable three-dimensional effects. The inflow conditions and the downstream pressure are provided for the computation. The calculation method is somewhat similar to that of Enseki,[5] but it incorporates major modifications suitable for internal flows. Enseki used Green's integral boundary-layer method[6] with a modified correlation for the entrainment function, which resulted in a physically unrealistic negative entrainment near the start of the interaction. The present analysis instead employs Green's integral lag-entrainment method,[7] which calculates the value of the entrainment function along with other unknowns. The treatment of the turning process of the flow between the shock and sonic point is modified in the present analysis to suit internal flows.

Comparisons of the solutions of the integral method with the experimental data[3] are made for interactions that are unseparated, near separation, and separated. For comparison purposes, solutions to the time-dependent, mass-averaged Navier-Stokes equations incorporating the two-equation Wilcox-Rubesin turbulence model are also presented from Ref. 3.

II. Analytical Flow Model

A typical wall pressure distribution for a normal shock wave/turbulent boundary-layer interaction is shown in Fig. 1. The start of interaction corresponds to the point at which an abrupt pressure rise begins. The upstream boundary for the calculation is at the start of the interaction where the experimental boundary-layer properties are specified. At the downstream boundary, the experimental value of static pressure is prescribed.

The boundary-layer development along the surface is divided into two regions (Fig. 1). Region I extends from the start of the interaction to the sonic point, as indicated by the wall pressure distribution. Experimental investigations[1,3,8,9] have shown that for transonic interactions, the start of the interaction is approximately five undisturbed boundary-layer thicknesses forward of the inviscid shock location. In the calculation method described here, the shock location is taken to be $5\delta_u$ downstream of the start of the interaction. However, the effect of varying the shock location on the wall pressure has been investigated and will be discussed in the section entitled Results and Discussion. In Region I, an integrated continuity equation, which is used along with Green's boundary-layer equations[7] rewritten in full axisymmetric form, permits free interaction between the inviscid stream and the boundary layer. The turning angle at the boundary-layer edge is assumed to be the result of a Prandtl-Meyer compression. Kooi[10] and East[11] have demonstrated that the supersonic compression upstream of the normal shock wave could be well represented by Prandtl-Meyer functions. However, this was not the case in the region between the normal shock wave and the sonic point. In this region, in which there exists an embedded supersonic flow, a much weaker compression takes place. Increased blockage in internal flows produces a larger embedded supersonic region than is found for interactions in planar flows.[3] The treatment of the turning process of the flow in this region is presented in the section entitled Auxiliary Functions for C_f and ν_{ref}.

Region II extends from the sonic point to the downstream boundary where the pressure is specified. In this region, viscous and inviscid flows are coupled by assuming one-dimensional inviscid flow based on the effective area of the duct. The boundary-layer equations used for Region I, along with the one-dimensional continuity equation, are employed to calculate the boundary-layer development in Region II. Downstream of the sonic point, flow blockage tends to produce small changes in the effective area of the duct and very mild streamline curvatures.[3,12] Based on this observation, it was decided that one-dimensional inviscid flow assumption should be a reasonable approximation for the inviscid flow in this region.

III. System of Equations

Boundary-Layer Equations

The compressible boundary-layer equation of Green's lag-entrainment method[7] have been rewritten in axisymmetric form. The momentum integral equation is

$$\left(1-\frac{\theta}{R}\right)\frac{d\theta}{dx}+\theta\left\{\frac{1}{u_e}\frac{du_e}{dx}\left[(H+2)-\frac{\theta}{2R}(H^2+2)\right]+\frac{1}{\rho_e}\frac{d\rho_e}{d_x}\left(1-\frac{\theta}{2R}\right)\right\}=\frac{C_f}{2} \tag{1}$$

where H, δ^*, and θ are the shape factor, displacement thickness, and momentum thickness, respectively. They are defined as

$$H=\delta^*/\theta,\quad \delta^*-\frac{\delta^{*2}}{2R}=\int_0^\delta\left(1-\frac{\rho u}{\rho_e u_e}\right)\left(1-\frac{y}{R}\right)dy,$$

$$\theta-\frac{\theta^2}{2R}=\int_0^\delta\frac{\rho u}{\rho_e u_e}\left(1-\frac{u}{u_e}\right)\left(1-\frac{y}{R}\right)dy$$

The equation for the streamwise rate at which mass is entrained into the boundary layer, called the entrainment equation, written in the axisymmetric form, is given by

$$(R-H_1\theta)\frac{dH_1}{dx}=(R-\delta)C_E-\left(RH_1\theta-\frac{H_1^2\theta^2}{2}\right)\frac{1}{\rho_e u_e}\frac{d\rho_e u_e}{dx}-(R-H_1\theta)H_1\frac{d\theta}{dx} \tag{2}$$

where H_1 is the shape factor and C_E is the entrainment coefficient representing the streamwise rate at which mass is entrained into the turbulent boundary layer. They are given by

$$H_1=\Delta/\theta \quad\text{and}\quad C_E=\frac{1}{2\pi(R-\delta)\rho_e u_e}\frac{d}{dx}\int_0^\delta 2\pi(R-y)\rho u\,dy$$

where Δ is the mass-flow thickness given by

$$\Delta-\frac{\Delta^2}{2R}=\int_0^\delta\frac{\rho u}{\rho_e u_e}\left(1-\frac{y}{R}\right)dy$$

after rearranging,

$$(R-\delta)^2=(R-\delta^*)^2+(R-\Delta)^2-R^2$$

The equation for the streamwise rate of change of entrainment coefficient, called the lag equation, is written as given by Green[7] (for $\gamma=1.4$)

$$\frac{dC_E}{dx}=\frac{F}{\theta}\left\{\frac{2\cdot 8}{H+H_1}\left[(C_\tau)_{\text{EQ}_0}^{1/2}-\lambda C_\tau^{1/2}\right]+\left(\frac{\theta}{u_e}\frac{du_e}{dx}\right)_{\text{EQ}}-\frac{\theta}{u_e}\frac{du_e}{dx}\left[1+0.075\,M_e^2\frac{(1+0.2M_e^2)}{(1+0.1M_e^2)}\right]\right\} \tag{3}$$

where empirical relationships for F, C_τ, λ, and equilibrium quantities are given in Ref. 7. λ is taken to be unity, which implies that the effects of any extraneous influences (e.g.,

freestream turbulence) are ignored. In the present analysis, the lag equation (3) has been retained in the planar two-dimensional form. It is felt that since the entrainment equation is written in full axisymmetric form, the lag equation, although developed for planar two-dimensional flows, should be applicable to axisymmetric flows. Earlier work by Ferrett and Lampard[13] has shown that the entrainment equation could be used in planar two-dimensional form for axisymmetric diffuser flows without loss of accuracy.

Equations (1), (2), and (3) represent differential equations for independent variables θ, H_1, and C_E. To express H_1 in terms of δ^* or θ, a transformed shape factor $\bar{H}$ is defined as

$$\bar{H}=\frac{1}{\theta}\left\{R-\left[R^2-2\int_0^{\delta}\frac{\rho}{\rho_e}\left(1-\frac{u}{u_e}\right)(R-y)\,dy\right]^{1/2}\right\}$$

Using the quadratic expression for static temperature for adiabatic boundary-layer flow

$$T=T_r+(T_e-T_r)\left(\frac{u}{u_e}\right)^2$$

and with $\rho/\rho_e=T_e/T$, we get from the expression for $\bar{H}$

$$R\delta^*-\frac{\delta^{*2}}{2}=\left(\frac{T_r}{T_e}-1\right)\left(R\theta-\frac{\theta^2}{2}\right)+\frac{T_r}{T_e}\left(R\bar{H}\theta-\frac{\bar{H}^2\theta^2}{2}\right) \quad (4)$$

where

$$\frac{T_r}{T_e}=1+r\frac{\gamma-1}{2}M_e^2$$

with r being the temperature recovery factor in adiabatic flow ($=0.9$). Equation (4) relates $\bar{H}$ to δ^* and θ. To relate H_1 to $\bar{H}$ (and thus to δ^* and θ), the empirical correlation from Green[7] is used:

$$H_1=3.15+\frac{1.72}{\bar{H}-1}-0.01(\bar{H}-1)^2$$

East[14] modified Green's correlation somewhat for application to separated flows. However, Green's correlation was used in the present analysis because it was tested against the measurements of Ref. 3 and the agreement was found to be very satisfactory.[15]

Equations Coupling Viscous and Inviscid Flows

The integrated continuity equation in axisymmetric form can be written as

$$\tan\phi=\frac{(R-\delta^*)}{(R-\delta)}\frac{d\delta^*}{dx}-\frac{1}{2}\left(\frac{R-\delta^*}{R-\delta}+1\right)\times(\delta-\delta^*)\frac{1}{\rho_e u_e}\frac{d\rho_e u_e}{dx} \quad (5)$$

where ϕ is the flow angle at the boundary-layer edge. Assuming a Prandtl-Meyer compression at the boundary-layer edge, $\phi=\nu_{ref}-\nu(M_e)$, where ν_{ref} is the reference for local Prandtl-Meyer turning and $\nu(M_e)$ is the Prandtl-Meyer function based on the local Mach number M_e. Equation (5) is used in Region I where the flow is supersonic at the boundary-layer edge. ν_{ref} is constant upstream of the shock but is modeled differently between the shock location and the sonic point. For Region II, where the flow is subsonic at the boundary-layer edge, the one-dimensional continuity equation for axisymmetric internal flow may be written as

$$\frac{d\delta^*}{dx}-\frac{(R-\delta^*)}{2}\frac{1}{\rho_e u_e}\frac{d\rho_e u_e}{dx}=0 \quad (6)$$

Forms of the System of Equations

Total pressure losses in the region just outside the boundary layer are typically very small for transonic normal shock interactions.[3,9,16] Neglecting this small loss in total pressure and assuming total temperature along the boundary-layer edge to be constant, we get

$$\frac{1}{\rho_e}\frac{d\rho_e}{dx}=-\frac{M_e^2}{M_e\{1+[(\gamma-1)/2]M_e^2\}}\frac{dM_e}{dx}$$

$$\frac{1}{u_e}\frac{du_e}{dx}=\frac{1}{M_e\{1+[(\gamma-1)/2]M_e^2\}}\frac{dM_e}{dx}$$

Using the above equations, Eqs. (1) through (4) and either Eq. (5) (Region I) or Eq. (6) (Region II) can be expressed as four ordinary differential equations for M_e, δ^*, θ, and C_E,

Region I:

$$\frac{dM_e}{dx}=\alpha_1,\quad \frac{d\delta^*}{dx}=\alpha_2,\quad \frac{d\theta}{dx}=\alpha_3,\quad \frac{dC_E}{dx}=\alpha_4 \quad (7)$$

Region II:

$$\frac{dM_e}{dx}=\beta_1,\quad \frac{d\delta^*}{dx}=\beta_2,\quad \frac{d\theta}{dx}=\beta_3,\quad \frac{dC_E}{dx}=\beta_4 \quad (8)$$

α_1, α_2, α_3, and α_4 are functions of M_e, δ^*, θ, C_E, C_f, and ν_{ref}, whereas β_1, β_2, β_3, and β_4 are functions of M_e, δ^*, θ, C_E, and C_f. The expressions for αs and βs can be found in Ref. 15. Before the above sets of equations can be solved, auxiliary expressions for C_f and ν_{ref} must be specified.

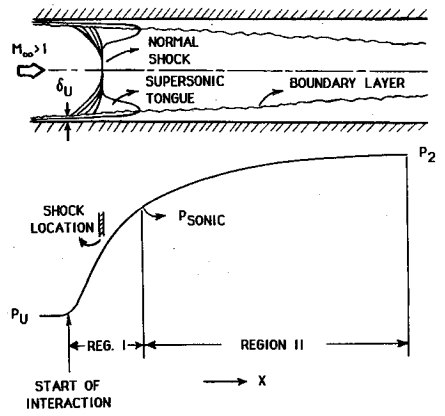

Fig. 1 Typical wall pressure distribution for a normal shock interaction.

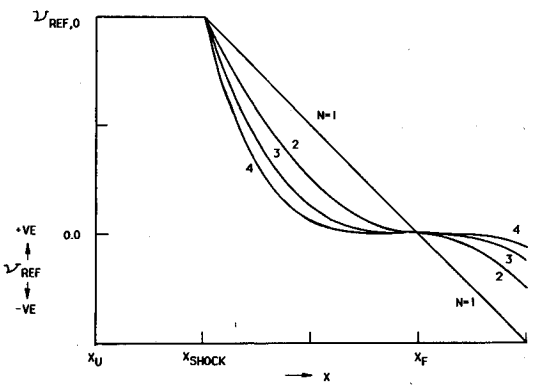

Fig. 2 ν_{ref} modeling.

Auxiliary Functions for C_f and ν_{ref}

The compressible skin-friction relation of Green[7] is used here. The skin-friction relation developed by Swafford[17] is also used for comparison. The kinematic shape factor H_K used in Swafford's skin-friction relation is related to $\bar{H}$ by Eq. (A5) of Green.[6] This equation was tested against the measurements of Ref. 3 and the agreement was found to be excellent.[15]

The specification of ν_{ref} represents the turning process of the flow at the boundary-layer edge. ν_{ref} is modeled as (Fig. 2):

$$\nu_{ref} = \nu_{ref,0}, \quad x_u \le x \le x_{shock}$$

$$= \nu_{ref,0}(1-\xi)^n, \quad x > x_{shock} \qquad (9)$$

where

$$\xi = \frac{x - x_{shock}}{x_F - x_{shock}}$$

Upstream of the shock wave, ν_{ref} is assumed to be constant and corresponds to M_e at the start of the interaction. This refers to the assumption of Prandtl-Meyer compression upstream of the shock wave. Downstream of the shock wave, where supersonic compression becomes much weaker, ν_{ref} is modeled as given by Eq. (9). Experiments[1,11] indicate that flow angle at the boundary-layer edge decreases sharply after the shock wave. This requires that ν_{ref} should decrease after the shock wave. The value of n is determined such that a continuous variation of $d\delta^*/dx$ is obtained between Regions I and II. The streamwise location where ν_{ref} becomes zero is determined by matching the calculated downstream pressure with the specified experimental pressure.

IV. Solution Procedure

With auxiliary functions C_f and ν_{ref} specified, Eqs. (7) and (8) represent four ordinary coupled first-order differential equations. The equations are solved by the fourth-order Runge-Kutta integration procedure. The initial values of M_e, δ^*, and θ for Region I are specified from the experiment. The initial value for C_E is determined from Eq. (A29) of Green[7] by assuming equilibrium conditions at the start of the interaction. The calculated values of δ^*, θ, M_e, and C_E at the end of Region I are used as the initial values for Region II. The integration of Eqs. (7) proceeds from the start of interaction until the sonic point is reached. Beyond the sonic point, the integration of Eqs. (8) is continued to the downstream location where the experimental pressure is prescribed.

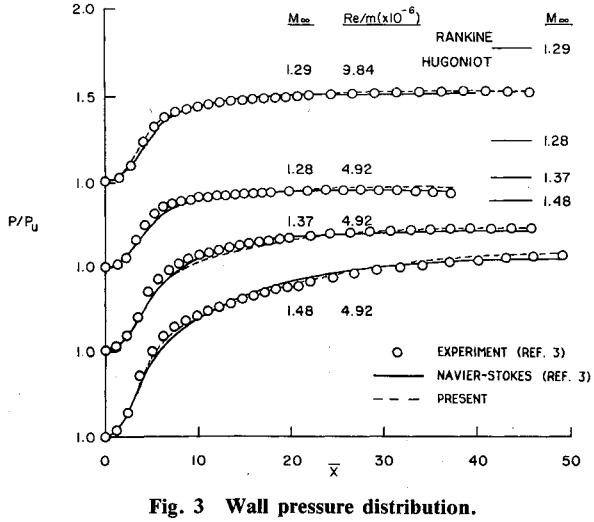

Fig. 3 Wall pressure distribution.

Three iteration procedures are required to complete the solutions. The first iteration determines the initial pressure perturbation required to start the interaction. The second iteration determines the streamwise extent of the ν_{ref} distribution which in turn determines the sonic point location. The third iteration determines the shape of the ν_{ref} distribution. The three iteration procedures are now described briefly.

Initial Pressure Perturbation

The integration of Eqs. (7) is started by applying a pressure perturbation to the flow at the boundary-layer edge in order to allow the boundary layer to interact with the inviscid flow. This was done by providing a positive perturbation to ν_{ref} as was done in Ref. 5. When the full expression for $\tan\phi$, Eq. (5), is used, the perturbation produces an increase in M_e in the downstream direction. This is the supercritical condition corresponding to that for laminar flows.[19] At supercritical conditions, Eqs. (7) do not describe the behavior of the boundary layer as observed in the experiments, where M_e decreases in the downstream direction. Der[19] has suggested why these equations may fail in this region. One reason may be the absence of normal pressure gradient terms in the boundary-layer equations. Another may result from the inadequacy of the single parameter H to describe the boundary layer.[20]

If the second term in the right-hand side of Eq. (5) is neglected, a positive perturbation to Eqs. (7) results in a decrease in M_e in the downstream direction, which is consistent with experiments. This is the subcritical condition.[18] Equation (5) then becomes

$$\tan\phi = \left(\frac{R-\delta^*}{R-\delta}\right)\frac{d\delta^*}{dx}$$

The above assumption implies that the viscous flow and the inviscid flow are coupled along the displacement edge. The coupling of the two flows in this fashion is known to work quite well for unseparated interactions. In fact, Kooi[10] found that such an assumption was valid for his separated transonic interactions. Moreover, the effect of blockage is to reduce the extent of separation for transonic interactions.[3] This further justifies the use of the above assumption for internal flows. The initial positive perturbation is taken to be the minimum ν_{ref} perturbation that produces a continuous supersonic compression at the boundary-layer edge. An iteration is required to determine the minimum ν_{ref}.

Sonic Point Location

The streamwise extent of ν_{ref} (i.e., location where it becomes zero) is determined by requiring the calculated downstream pressure to match with the specified experimen-

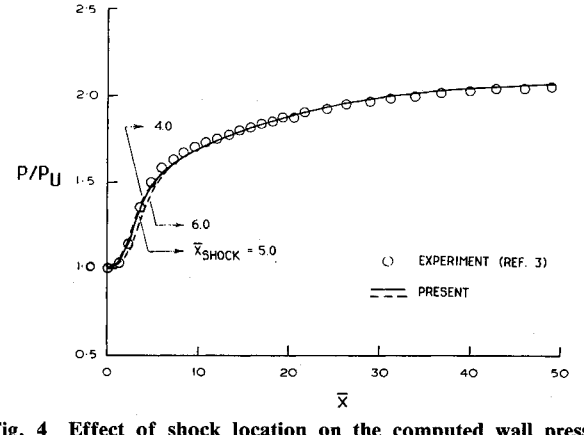

Fig. 4 Effect of shock location on the computed wall pressure: $M_\infty = 1.48$, $Re/m = 4.92 \times 10^6$.

tal pressure. This in turn determines the sonic point. The procedure is as follows. For a particular value of n, the location of $\nu_{ref}=0$ is initially set far downstream. An initial pressure perturbation is provided to the set of Eqs. (7), and integration is performed until the sonic point is reached. Thereafter, the set of Eqs. (8) is solved up to the location where experimental pressure is prescribed. If the calculated pressure does not match the experimental value, the $\nu_{ref}=0$ location is changed to a point farther upstream, and the calculations are repeated. Iteration is required to match the calculated downstream pressure with the experimental value.

Shape of the ν_{ref} Distribution

Initially the solution of the interaction is obtained with exponent n in the ν_{ref} model equal to 1. If a continuous variation of $d\delta^*/dx$ between Regions I and II is not obtained, the value of n is increased until the above condition is satisfied. For the transonic interaction data of Ref. 3, the optimum value of n was found to be equal to 3.

The calculations presented here were performed on the Cyber 170-750 computer at the University of Washington. For the second and third types of iteration discussed earlier, the results of each iteration were saved to provide a better estimate for the next iteration. As an example of the speed of the program, the computing time varied from approximately 5 CPUs to 8 CPUs (for different test cases) for a particular value of n and a particular location of $\nu_{ref}=0$. For a particular value of n, 6 to 8 iterations were required to determine the $\nu_{ref}=0$ location that matches the calculated pressure with the downstream experimental pressure.

V. Results and Discussion

The computed integral properties of the boundary layer from the viscous-inviscid integral method are presented for the test cases of Ref. 3 in conjunction with the results of Navier-Stokes simulation from Ref. 3. In Ref. 3, a normal shock wave generated in a constant-area circular duct interacted with the turbulent boundary layer developing on the wall of the duct. The freestream Mach number was varied from 1.28 to 1.48, causing the flow to be unseparated, near separation, and separated.

Figure 3 shows the wall pressure distribution for the interaction at different Mach numbers and Reynolds numbers. $\bar{X}$ is measured from the start of the interaction and is normalized by the boundary-layer thickness at the start of the interaction. The integral computations agree very well with the experimental wall pressure distribution throughout the interaction, as do the Navier-Stokes predictions. Figure 4 shows the effect of different assumed shock wave locations on the wall pressure distribution for the freestream Mach number of 1.48. The overall pressure distribution is not altered significantly, implying that the solution is rather insensitive to small changes in the assumed shock wave location.

The skin-friction distributions calculated with the integral method agree well with the experimental skin friction except in the neighborhood of the shock wave (Fig. 5). The calculated skin-friction levels are higher than the experimental values just upstream of the shock wave. For $M_\infty=1.48$, the calculated separation length is much smaller than that observed in the experiment. The equilibrium locus used in the lag equation is simply an algebraic extension of the locus for attached turbulent flows and thus may have its limitation for turbulent separated flows.[14] The skin-friction relation of Green[7] may also have its limitation for flows subjected to such abrupt adverse pressure gradients. For comparison, the results obtained for $M_\infty=1.48$ using Swafford's[17] skin-friction relation are shown in Ref. 15. The difference in skin friction using the two different skin-friction relations is small.

Displacement and momentum thicknesses computed from the integral method are shown in Figs. 6 and 7, respectively. The agreement with experimental data is very good at the lower freestream Mach numbers where the flow is unseparated. As the freestream Mach number increases and the flow becomes increasingly separated, the comparisons are not quite as good as for the unseparated interactions, although δ^* and θ distributions, obtained with such a simple integral analysis are comparable to the results obtained with the Navier-Stokes simulation.

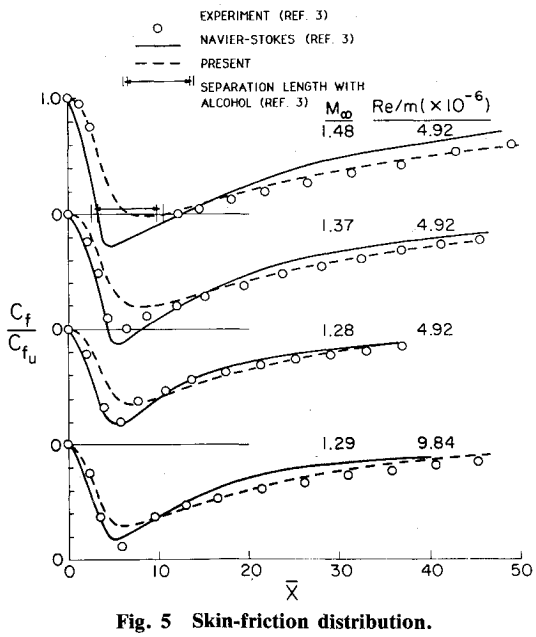

Fig. 5 Skin-friction distribution.

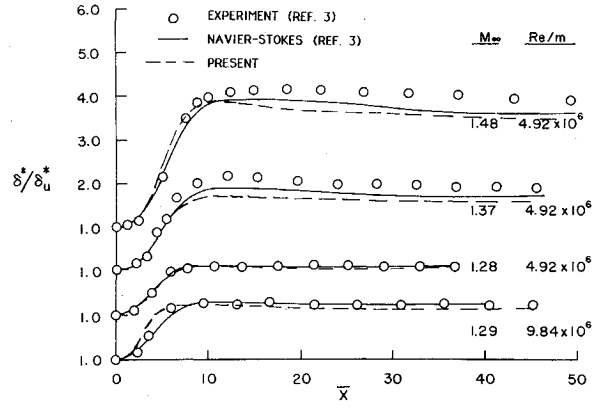

Fig. 6 Displacement thickness distribution.

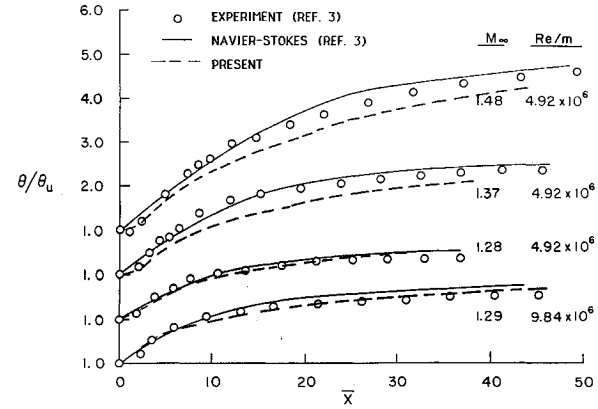

Fig. 7 Momentum thickness distribution.

When the ratio of the upstream boundary-layer thickness to the duct radius becomes moderately large, multiple shock wave/boundary-layer interactions may occur in the duct.[21] Thus, the upper limit on the value of δ_u/R, for which the present analysis is applicable, is dictated by the formation of the multiple shock interactions. The analysis will also not apply to flows with strong streamline curvature where quasi-one-dimensional assumption may not be adequate (e.g., curved ducts).

VI. Concluding Remarks

An approximate integral viscous-inviscid interaction method may be used to calculate the development of a turbulent boundary layer subjected to a normal shock wave in an internal flow. An analytical model is postulated for the coupling of the inviscid flow with Green's integral lag-entrainment boundary-layer method. With this direct coupling, the equations are integrated simultaneously. Comparisons of the calculated results with experimental data show good agreement for unseparated interactions and reasonable agreement with the trend of the viscous effects when the interaction becomes increasingly separated.

Acknowledgments

This work was supported by NASA Grants NGR-48-002-047 and NGR-48-002-141 under the administration of the Aerodynamics Branch, Ames Research Center.

References

[1]Seddon, J., "The Flow Produced by Interaction of a Turbulent Boundary Layer with a Normal Shock Wave of Strength Sufficient to Cause Separation," ARC R & M No. 3502, March 1960.

[2]Mateer, G. G. and Viegas, J. R., "Effect of Mach and Reynolds Numbers on a Normal Shock Wave/Turbulent Boundary Layer Interaction," AIAA Paper 79-1052, July 1979.

[3]Om, D., Viegas, J. R., and Childs, M.E., "Transonic Shock-Wave/Turbulent Boundary-Layer Interactions in a Circular Duct," AIAA Journal, Vol. 23, May 1985, pp. 707-714, (also see AIAA Paper 82-0990).

[4]"Computation of Viscous-Inviscid Interactions," AGARD-CPP-291, Colorado Springs, Sept. 1980.

[5]Enseki, F. K., "A Calculation Method for the Turbulent Transonic Viscous-Inviscid Interaction on Airfoils," AIAA Paper 72-5, Jan. 1972.

[6]Green, J. E., "The Prediction of Turbulent Boundary Layer in Compressible Flow," *Journal of Fluid Mechanics,* Vol. 31, Pt. 4, 1968, pp. 753-758.

[7]Green, J. E., Weeks, D. J., and Brooman, J. W. F., "Prediction of Turbulent Boundary Layers and Wakes in Compressible Flow by a Lag-Entrainment Method," ARC R&M No. 3791, Jan. 1973.

[8]Gadd, G. E., "Interactions Between Normal Shock Waves and Turbulent Boundary Layers," ARC R&M No. 3262, Feb. 1961.

[9]Kooi, J. W., "Experiment on Transonic Shock-Wave Boundary Layer Interaction," AGARD Conference on Flow Separation, AGARD-CPP-168, Paper No. 30, 1975.

[10]Kooi, J. W., "Influence of Free-Stream Mach Number on Transonic Shock Wave Boundary Layer Interaction," Symposium on Transonic Configurations, NLR-MP-78013-U, June 1978.

[11]East, L. F., "The Application of a Laser Anemometer to the Investigation of Shock-Wave Boundary Layer Interactions," AGARD Conference on Applications of Non-Intrusive Instrumentation in Fluid Flow Research, AGARD-CP-193, 1976.

[12]Mateer, G. G., Brosh, A., and Viegas, J. R., "A Normal Shock-Wave Turbulent Boundary Layer Interaction at Transonic Speeds," AIAA Paper 76-161, July 1976.

[13]Ferrett, E. F. C. and Lampard, D., "A Calculation Method for the Pressure Recovery Produced by Diffusers Fitted with Tailpipes," Proceedings of the Symposium on Internal Flows, University of Salford, England, April 1971.

[14]East, L. F., Smith, P. D., and Merryman, P. J., "Prediction of the Development of Separated Turbulent Boundary Layers by the Lag-Entrainment Method," RAE Tech. Rept. 77046, March 1977.

[15]Om, D. and Childs, M. E., "An Integral Analysis of Transonic Normal Shock Wave/Turbulent Boundary Layer Interactions in Internal Flow," Mechanical Engineering Technical Report ME TR-82-GA-12-1, University of Washington, Seattle, Dec. 1982.

[16]Ackeret, J., Feldman, F., and Rott, N., "Investigation of Compression Shocks and Boundary Layers in Gases Moving at High Speeds," NACA TM 1113, Jan. 1947.

[17]Swafford, T. W., "Analytical Approximation of Two-Dimensional Separated Turbulent Boundary-Layer Velocity Profiles," Arnold Air Force Station, Tenn., AEDC-TR-79-99, Oct. 1980.

[18]Klineberg, J. M. and Lees, L., "Theory of Laminar Viscous-Inviscid Interactions in Supersonic Flow," *AIAA Journal*, Vol. 7, Dec. 1969, pp. 2211-2221.

[19]Der, J. J., "Theoretical Study of the Separation of Subcritical and Supercritical Turbulent Boundary Layers by the Method of Integral Equations," AIAA Paper 69-34, 1969.

[20]Bradshaw, P., "Turbulent Boundary Layers," *The Aeronautical Journal of the Royal Aeronautical Society*, Vol. 72, May 1968, pp. 451-459.

[21]Om, D. and Childs, M. E., "An Experimental Investigation of Multiple Shock Wave/Turbulent Boundary Layer Interactions in a Circular Duct," AIAA Paper 83-1744, July 1983 (accepted for publication in *AIAA Journal*).